Indonesian Journal of Electrical Engineering and Computer Science
Vol. 36, No. 3, December 2024, pp. 1605~1612
ISSN: 2502-4752, DOI: 10.11591/ijeecs.v36.i3.pp1605-1612

A hybrid classification approach for automatically recognizing COVID-19 using deep transfer learning using chest radiographs

Murthuja Pinjara, Anjan Babu G.
Department of Computer Science, Sri Venkateshwara University, Tirupathi, India

Article Info

Article history:

Received Mar 15, 2024
Revised Jul 23, 2024
Accepted Jul 29, 2024

Keywords:

Convolution neural network
COVID-19
Edge oriented histogram
Local binary pattern
Support vector machine
Transfer learning
X-ray images

ABSTRACT

Coronavirus 2019 causes COVID-19, a worldwide epidemic. It endangers millions globally. Early illness detection improves recovery and control. X-ray image processing is used to categorise and identify COVID-19 in the present study. Preprocessing, feature extraction using local binary pattern (LBP) and edge orient histogram (EOH), and classification utilising K-nearest neighbour (KNN), Navie Bayes, support vector machine (SVM), and transfer learning convolution neural networks (CNNs) are some of the stages that are implemented in the process. Other phases in the process include preprocessing, feature extraction, and preprocessing. LBP+KNN, EOH+KNN, LBP+SVM, EOH +SVM, CNN+LBP, and CNN+EOH are the outputs derived from the combinations of feature extraction operators and classifiers. Other possible outcomes are CNN+EOH and CNN+LBP. A total of 4,000 pictures were used as the basis for conducting an analysis of the performance of six different models. In order to train the models, 10-fold cross-validation was used, and their accuracy was measured accordingly. The evaluation results indicate a high level of accuracy in diagnosis, ranging from 90.2% to 97.56%. The CNN+LBP and CNN+EOH models have demonstrated superior performance compared to other models, achieving average accuracies ranging from 96.66% and 98.54%.

Corresponding Author:

Murthuja Pinjara
Department of Computer Science, Sri Venkateshwara University
Tirupathi, Andhra Pradesh, 517502, India
Email: pmurthuja.mca@hotmail.com

1. INTRODUCTION

Human respiratory tract infections may be caused by the pandemic virus coronavirus 2019 (COVID-19). The city of Wuhan in China was hit hard by this outbreak in December 2019, killing millions. COVID-19 has to be identified quickly since it is a threat to world health [1]. Thus, it is critical to aid in the early detection of this sickness, forecast the patient's recovery day, and provide assistance to the doctors who make the diagnostic [2]. Although the virus has infected a large number of individuals, the percentage of those in a critical or severe condition is very low [3]. As COVID-19 instances rise, the need for intensive care facilities is also increasing. This growth is putting a strain on the healthcare system. Researchers are using medical imaging techniques such as computed tomography (CT) scans and X-rays to search for symptoms of the new coronavirus [4]. These methods also do not provide a unique way to categorise the virus in tiny areas of the images.

When doing COVID-19 testing in epidemiological areas, researchers involved in several recent studies use chest radiography as a diagnostic tool. According to their findings, the study of radiographic pictures has the potential to serve as an alternative to the polymerase chain reaction (PCR) method since it demonstrates a better level of sensitivity in some instances. With the purpose of screening the coronavirus COVID-19 for two classes of normal pneumonia, in spite of the significant advancements that have been made in recent times, the identification of COVID-19 continues to be challenging owing to a wide range of obstacles, including enhancements in lighting and accessories.

Although partial occlusions and machine deflection of contaminated regions are being captured, the identification rate continues to be poor. This is because of the effect of varying ambient conditions as well as variances in the characteristics of specific machines. Through the use of deep learning and, more particularly, convolutional neural networks, it is possible to recover and learn a great deal of information that may be used to develop an effective detection system. As a consequence of this, the framework for machine learning need to concentrate just on the most significant parts of the face, while not being too sensitive to the other areas of the face. Features that were handcrafted for the purpose of detecting COVID-19 assignments are no longer sufficient. Deep learning approaches have the potential to provide a solution to these issues yet it may not be the best one. Convolutional neural network (CNN) has achieved a great deal of success in the majority of the domains of machine learning and computer vision. Researchers utilise CNN for object recognition in a broad variety of applications [5], [6]. The purpose of this research is to offer a method for identifying COVID-19 that is based on deep learning and takes into consideration the observation that came before it. There are three basic categories that may be used to classify features: appearance, geometry, and motion characteristics, in that order. There are a number of appearance features that are used rather often, including pixel intensity [7], Gabor texture [8], LBP [9], and histogram of oriented gradients (HOG) [10]. These characteristics were taken into consideration from the whole inficted area.

When compared to earlier attempts, all of the prior investigations have achieved significant progress in the identification of COVID-19; nevertheless, they do not have a clear strategy for identifying and detecting the virus. With the help of a combined features network-based architecture, we make an effort to find a solution to this problem by concentrating on the minute regions of X-ray and CT images, aiming for an accuracy that is comparable to that of the standard publicly accessible dataset. The challenges of characteristics feature extraction via the use of local binary pattern (LBP) and edge orient histogram (EOH), as well as classification through the use of K-nearest neighbour (KNN), Navie Bayes, support vector machine (SVM), and transfer learning CNNs, are the primary topics of discussion in this study. There are a number of other procedures that are included into the process. Some of these activities include preprocessing, function extraction, and processing. The outputs that are derived from the combinations of feature extraction operators and classifiers are as follows: CNN+LBP, CNN+EOH, LBP+KNN, EOH+KNN, LBP+SVM, and EOH+SVM. CNN+LBP is the combination that produces the most accurate results. The CNN+EOH and CNN+LBP outcomes are two more possibilities that might take place. Significant future improvements are still to come. There was a great deal of success with the live, real-time testing of the system. In light of the fact that the GPU and hardware implementation for real time classification in infected area by taking average surface distance method to calculate infected area show the average ranges in normal and abnormal ranes in using hardware implementation.

The structure of our analysis is as described below. Introduction surveys of proposed features extraction are discussed in section 2. Section 3 discusses the model that has been offered. An announcement has been made on the test results and interpretation for section 4. In the section 5, the concluding statement is presented.

2. FEATURE EXTRACTION METHODS

The process of acquiring spatial characteristics, which is carried out throughout the whole of the image itself. In contrast to the conventional methods, which involve breaking down the affected region of the picture into its constituent parts before carrying out an analysis, the following are some techniques for feature extraction that are discussed below.

2.1. Local binary pattern

LBP is used to extract unique image features without overlap. The first step is to split the image into sections using user-defined uniform blocks. To compute an LBP value, identify the centre pixel of each patch and compare it to its neighbour pixel situated around it. The Gabor filter is often a bandpass filter that is created by multiplying the odd and even filters that are given in (1). The output bit that is assigned to mi is determined by the function f(x), and if f(x) is more than zero, then a '1' is assigned; otherwise, if f(x) is equal to or less than zero, then a '0' is assigned. After evaluating all nearby pixels, the 8 bits are combined starting with the top left corner to generate a pattern.

$$LBP_i = \sum_{i=0}^{m-1} f(m_i - m_c)2^i \quad (1)$$

2.2. Edge orientation histogram

In order to generate a feature in an image that is composed of gradients all across the picture, the HOG algorithm is a method that may be taken advantage of. EOH, on the other hand, is an alternative to HOG that is much more time-efficient and transparent. It is a well-known approach that may be used to recognise [11], and it is advantageous in circumstances when there is a limitation on the amount of time or memory that is available. First, the image is converted to grayscale. Then it separates the image into I(x,y) blocks. The Sobel method is used to calculate the horizontal (Gx) and vertical (Gy) edges in (2) and (3). Edge operators (Kx and Ky) fetch block edges. This is done to calculate horizontal (Gx) and vertical (Gy) edges. In (4) and (5) display the angle theta and strength S(x, y) of the edge orientation after computation and positioning in polar coordinates. Previous computations yielded these equations. Next, split the angles and strengths into N bins to obtain the EOH feature. Using blocks with the EOH operator allows for picture reorientation, since the highest bin value is always at θ degrees. This method is good at finding borders and resists fluctuations in light intensity. In a photograph, large gradients in opposing directions may create a corner.

$$G_{(x)}(x,y) = K_x I(x,y) \tag{2}$$

$$G_{(y)}(x,y) = K_y I(x,y) \tag{3}$$

$$\theta = \arctan\left(\frac{G_y(x,y)}{G_x(x,y)}\right) \tag{4}$$

$$S(x,y) = \sqrt{G_{X^2}(x,y) +} \sqrt{G_{Y^2}(x,y)} \tag{5}$$

3. PROPOSED MODEL

This paper presents a novel method for the identification of COVID-19 by using a hybrid feature extraction method that makes use of transfer learning in conjunction with a CNN network. First, features are extracted from LBP, then features are extracted from EOH, and lastly, diverse outputs are fused together. These are the phases that make up the proposed technique. Identification of normal and pneumonia with the assistance of the model that has been developed. An illustration of the full process may be seen in Figure 1. There are X-ray photographs that are used in benchmarking datasets [12], [13], and actual situations might differ in rotation even for the same topic.

Within the framework of our design, we want to modify the precision of the COVID-19 classification using contemporary convolutional network architecture. This includes grayscale photos as well as photographs with LBP and EOH characteristics. Following the addition of each convolution layer, activations of rectified linear unit (ReLu) are added, and soft-max classifiers are used for the activation function in the flattening layer. As can be seen in Table 1, the first stage of feature extraction from LBP and EOH features is accomplished via the use of a transfer learning CNN design. Next, we have KNN and SVM classifiers, which include both features such as LBP and EOH. Finally, we have Naive Bayes with image classification, which has a dropout ratio of 0.2, 64 dense layers of ReLU architecture, and two activation points. The deployment of the Softmax classifier consists of the same. A pre-processing phase is performed on the grayscale pictures that are entered during the training stage. Table 2 is a compendium of the various other performance metrics that are available. Any size of input image can be accepted by the transfer learning CNN before the average polling algorithm is applied to the image that is being input. During the optimization stage, we employ a variety of optimizers, including SGD, RMS, and Adam. Among all of the optimizers, Adam has the most accurate comparison to what we use in comparative shown in Table 3. This step involves conducting strength normalisation and scaling on the pixel values. The pictures in concern are provided as input.

This is very necessary in order to avoid a scenario of over-fitting. Additionally, the model is made simpler to optimise when the convexity of the objective function is increased at a higher level. One of the factors that determines the appropriate rate of weight decay is the total number of batches that are performed and the number of weight updates. During the course of our empirical study on Adam, we discovered that the duration and the number of batch runs are extended in proportion to the optimal weight decay being smaller. In order to minimise the amount of weight change fluctuations that occur over the course of subsequent cycles, momentum is used, and its starting value was set to zero.

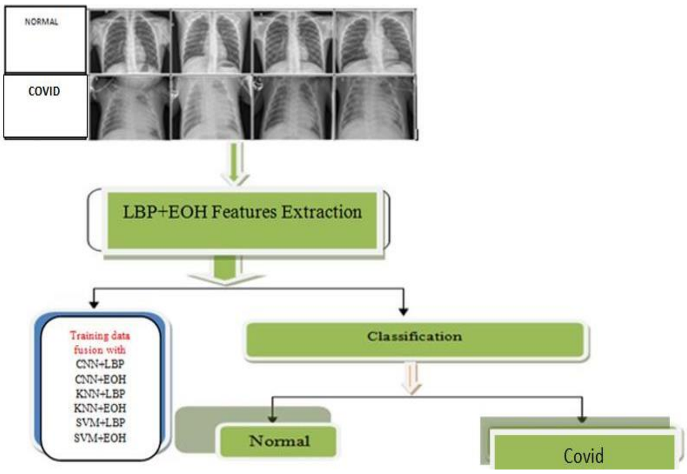

Figure 1. Proposed model

Table 1. Proposed CNN architecture

Layer	Filter	Kernel Size	Stride	Padding	Activation
Conv (C1)	64	5	1	2	ReLU
Pooling		3	2	0	
Conv (C2)	32	5	1	2	ReLU
Pooling		3	2	0	
Conv (C3)	64	5	1	2	ReLU
Pooling		3	2	0	
Fully connected layer (FC4)					Softmax

Table 2. Performance metric parameters

Performance measure	Transfer learning CNN
Batch size	32
Image input dimension	224×224
Optimizer	Adam
Activation function	ReLu
Loss function	Categorical cross entropy

Table 3. Optimizers loss and accuracy comparison analysis

Optimizer	Loss	Accuracy (%)
SGD	0.6826	0.68
RMS	0.4448	0.86
Adam	0.3945	0.91

The proposed model implementation by using unsupervised learning algorithm, an unsupervised learning algorithm is a type of machine learning algorithm designed to find patterns, structures, or relationships in data without the need for labeled examples or explicit instructions on what to look for. Unlike supervised learning, where the model is trained on input-output pairs, unsupervised learning deals with data that has no corresponding output labels. The goal is to uncover hidden structures, such as clusters, associations, or dimensionality reductions, within the data. The outcome of an accuracy (%) can be followed by a following step to be needed.

- Step 1: Load the dataset [14]
- Step 2: Split the dataset tanning and testing
- Step 3: Apply the preprocessing technique
- Step 4: Two set of features such as LBP, and EOH are extracted from Chest MRIs, and then these features are used in classifier CNN with transfer learning
- Step 5: The combined set of features, i.e. CNN+LBP, and CNN+HOG, contributed 96.66% accuracy and 98.54%
- Step 6: The proposed method gives very good performance even with a small dataset, and it is comparable to the deep learning approach combination of LBP and EOH features with transfer learning of CNN

The novel aspect of the proposed methodology is that it combines features such as LBP and EOH with transfer learning of CNN, which is a procedure in which the resulting output picture is more informative and comprehensive than any of the input of the picture. This is accomplished by combining relevant information from a set of images into the individual picture. This methodology has the potential to enhance the quality of the application data. Utilizing the merging approach allowed for the integration of choices made by CNN+LBP and CNN+EOH. Because LBP is able to record local texture patterns, it is well suited for tasks such as discriminating between various surface textures in materials and identifying minor changes in input characteristics. Through the process of comparing each pixel with the pixels that are next to it, it is made of relative values. The extraction of EOH characteristics allows for the representation of a depth (Z) sequence from a variety of various viewpoints. It is possible to fuse these characteristics by considering decision-level fusion. In this particular instance, it is important to emphasize that feature-level fusion could be used. However, the feature-level fusion process is not compatible with many feature sets and high dimensionality, despite the fact that it is basic. This demonstrates that multimodal combination characteristics provide a highly effective method of enhancing accuracy rates, which was the initial strategy that was recommended. In contrast to the advanced image handling techniques, such as planned architectures for real-time environments, however, significant future improvements are still to come. There was a great deal of success with the live, real-time testing of the system. In light of the fact that the Jetson Nano GPU hardware has modest power consumption, the decisions that were made were satisfactory [15].

4. EXPERIMENTAL RESULTS AND ANALYSIS

Within the framework of the Tensor flow system, we put the suggested model through its paces on the Google Colab platform, which is running on the Windows internet. For the purpose of detecting COVID utilising X-ray chest pictures, datasets that are accessible to the public are used. All of the findings are shown in Figures 2 and 3, respectively. The accuracy curve is shown in red, while the loss curve is displayed in green. Additionally, the loss is stabilised after 10 to 30 epochs, and their test results are also displayed. The suggested model architecture, such as CNN+LBP and CNN+EOH, has a consequent accuracy of 96.66% and 98.54%, respectively, when it comes to the average accuracy of recognition. In addition, we evaluate the accuracy of our procedure by analysing chest X-ray pictures obtained from a single channel examination. Using our methods, we examine whether or not it is feasible. Histogram of directed gradients, SVM, and KNN are some of the elements that contribute to our approach's increased efficiency when compared to other CNN-related methodological methods. The advantage of our technique is achieved by making effective use of the complements of a number of different X-ray chest image sources. In Table 4, we provide comparisons between our method and the other methods that are considered to be state-of-the-art for the categorization of X-ray chest imaging pictures and also bargargh representation for existing and proposed models (green) architectures are shown in Figure 4.

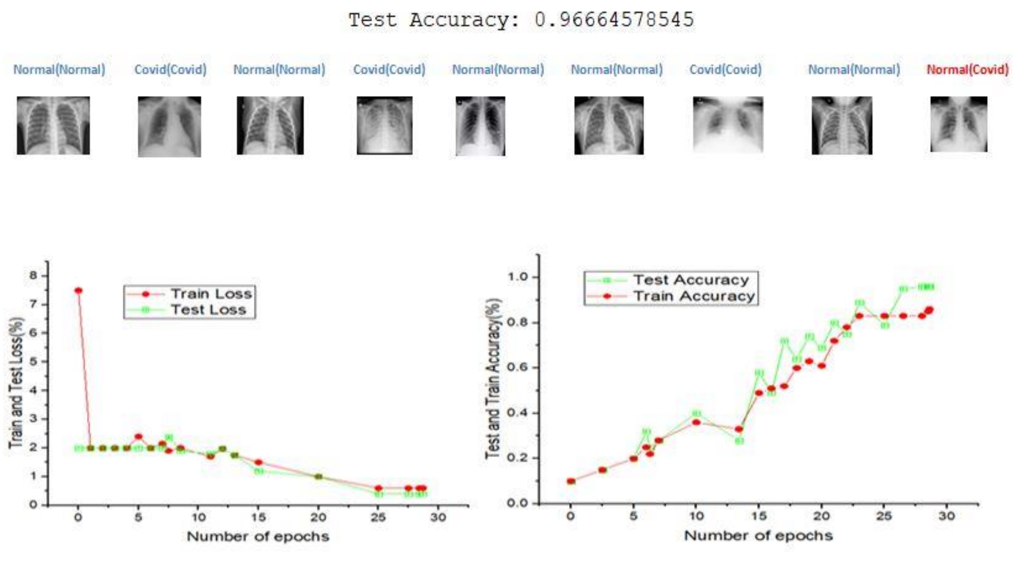

Figure 2. Training and test loss accuracy and validation loss, and their test analysis test results for CNN+LBP. Number of epochs in x axis, train and test loss, their accuracy (%) in y axis

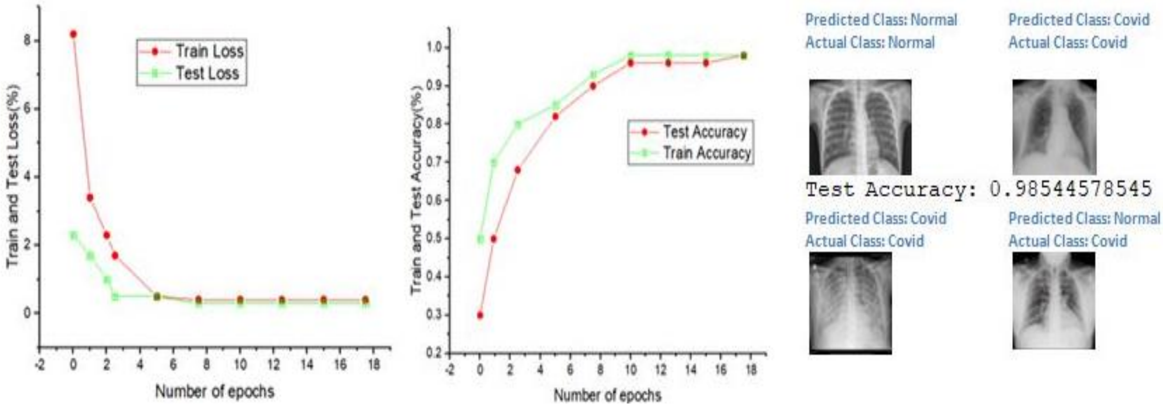

Figure 3. Training and test loss accuracy and validation loss, and their test analysis test results for CNN+EOH. Number of epochs in x axis, train and test loss, their accuracy (%) in y axis

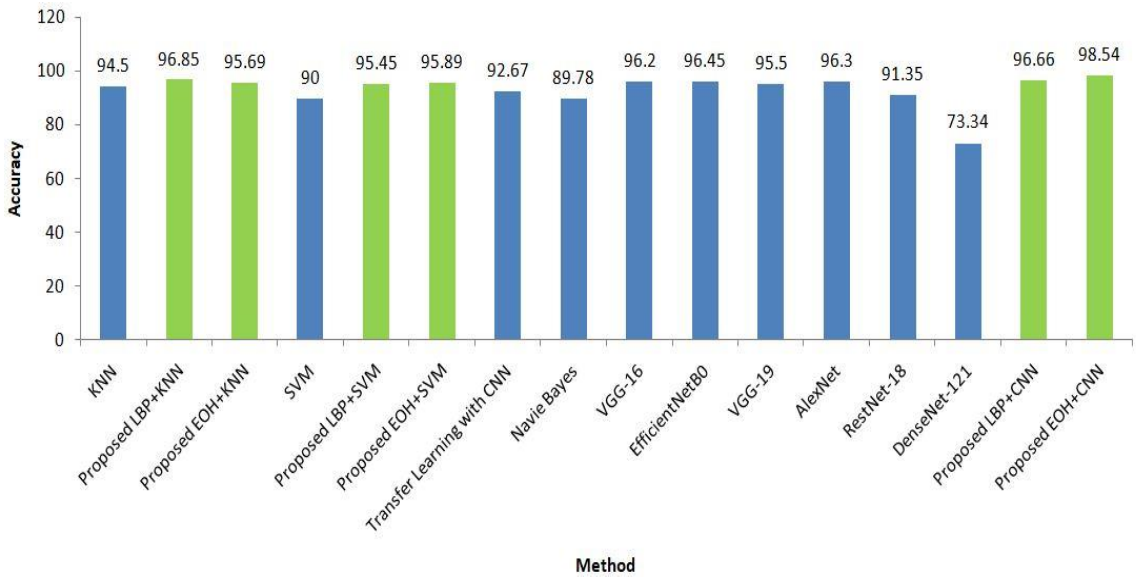

Figure 4. Bargargh representation for existing and proposed models architectures

Table 4. Comparison and contrast, it is empirical that the proposed classification techniques

Method	Accuracy (%)	Accuracy (%) for Proposed architectures
KNN [16]	94.50	
Proposed LBP+KNN		**96.85**
Proposed EOH+KNN		**95.69**
SVM [17]	90.00	
Proposed LBP+SVM		**95.45**
Proposed EOH+SVM		**95.89**
Transfer learning with CNN [18]	92.67	
Navie Bayes [19]	89.78	
VGG-16 [20]	96.20	
EfficientNetB0 [21]	96.45	
VGG-19 [22]	95.50	
AlexNet [23]	96.3	
RestNet-18 [24]	91.35	
DenseNet-121 [25]	73.34	
Proposed LBP+CNN		**96.66**
Proposed EOH+CNN		**98.54**

5. CONCLUSION

By analyzing the images of the chest X-rays and putting them into the model, deep learning has the potential to be a very valuable tool in the medical business for illness identification. Normal and COVID-19 were among the first categories into which the chest X-rays were placed. An accuracy range of 90% to 94.5% was attained using the pre-existing model for categorization. The next step was to differentiate between the many suggested feature combinations based on the underlying architectures, such as LBP+KNN, EOH+KNN, LBP+SVM, EOH+SVM, CNN+LBP and CNN+EOH. We successfully attained a grater accuracy of 98.54% using CNN+EOH. As a proof of concept, we demonstrated that COVID-19 X-rays may be categorized into severe, mild, and medium stages according to the severity of the virus. The CNN+EOH combination achieved the best results for severity classification, with an accuracy gain of 4%.Our suggested methodology allows for the efficient identification of COVID-19 by mass screening of individuals. When compared to the more traditional RT-PCR approach, it will help provide more rapid and precise findings at a lower cost. Hospitals often have X-ray machines since they are essential pieces of medical equipment. That way, people in such places may also have access to this diagnostic therapy. Consequently, a cutting-edge model is required for real-time applications in order to reduce training time and delivery. Future efforts will focus on streamlining the network and speeding up the algorithm.

REFERENCES

[1] L. Wynants *et al.*, "Prediction models for diagnosis and prognosis of COVID-19: systematic review and critical appraisal," *bmj*, vol. 369, 2020.

[2] D. Uphade and A. Muley, "Identification of parameters for classification of COVID-19 patient's recovery days using machine learning techniques," *Journal of Mathematical and Computational Science*, 2022, doi: 10.28919/jmcs/7062.

[3] L. Yan *et al.*, "Prediction of criticality in patients with severe COVID-19 infection using three clinical features: a machine learning-based prognostic model with clinical data in Wuhan," *MedRxiv*, 2020.

[4] A. S. Al-Waisy *et al.*, "COVID-DeepNet: hybrid multimodal deep learning system for improving COVID-19 pneumonia detection in chest X-ray images," *Computers, Materials and Continua*, vol. 67, no. 2, pp. 2409–2429, 2021, doi: 10.32604/cmc.2021.012955.

[5] A. Krizhevsky, I. Sutskever, and G. E. Hinton, "ImageNet classification with deep convolutional neural networks," *Communications of the ACM*, vol. 60, no. 6, pp. 84–90, 2017, doi: 10.1145/3065386.

[6] M. Shaha and M. Pawar, "Transfer learning for image classification," in *Proceedings of the 2nd International Conference on Electronics, Communication and Aerospace Technology, ICECA 2018*, Mar. 2018, pp. 656–660, doi: 10.1109/ICECA.2018.8474802.

[7] M. R. Mohammadi, E. Fatemizadeh, and M. H. Mahoor, "PCA-based dictionary building for accurate facial expression recognition via sparse representation," *Journal of Visual Communication and Image Representation*, vol. 25, no. 5, pp. 1082–1092, Jul. 2014, doi: 10.1016/j.jvcir.2014.03.006.

[8] C. Liu and H. Wechsler, "Gabor feature based classification using the enhanced Fisher linear discriminant model for face recognition," *IEEE Transactions on Image Processing*, vol. 11, no. 4, pp. 467–476, Apr. 2002, doi: 10.1109/TIP.2002.999679.

[9] C. Shan, S. Gong, and P. W. McOwan, "Facial expression recognition based on local binary patterns: A comprehensive study," *Image and Vision Computing*, vol. 27, no. 6, pp. 803–816, May 2009, doi: 10.1016/j.imavis.2008.08.005.

[10] U. Dudekula and N. Purnachand, "Linear fusion approach to convolutional neural networks for facial emotion recognition," *Indonesian Journal of Electrical Engineering and Computer Science*, vol. 25, no. 3, pp. 1489–1500, Mar. 2022, doi: 10.11591/ijeecs.v25.i3.pp1489-1500.

[11] M. Mukeshimana, A. Niyongere, and J. Ndikumagenge, "Facial emotion recognition feature extraction: a survey," in *Emotion Recognition - Recent Advances, New Perspectives and Applications*, IntechOpen, 2023.

[12] L. Wang, Z. Q. Lin, and A. Wong, "COVID-Net: a tailored deep convolutional neural network design for detection of COVID-19 cases from chest X-ray images," *Scientific Reports*, vol. 10, no. 1, Nov. 2020, doi: 10.1038/s41598-020-76550-z.

[13] S. Albahli, "A deep neural network to distinguish COVID-19 from other chest diseases using X-ray images," *Current Medical Imaging Reviews*, vol. 17, no. 1, pp. 109–119, 2022, doi: 10.2174/18756603mta3nmtac5.

[14] S. Kumar and A. Mallik, "COVID-19 detection from chest X-rays using trained output based transfer learning approach," *Neural Processing Letters*, vol. 55, no. 3, pp. 2405–2428, Oct. 2023, doi: 10.1007/s11063-022-11060-9.

[15] U. Dudekula and N. Purnachand, "Analysis of facial emotion recognition rate for real-time application using NVIDIA Jetson Nano in deep learning models," *Indonesian Journal of Electrical Engineering and Computer Science*, vol. 30, no. 1, pp. 598–605, Apr. 2023, doi: 10.11591/ijeecs.v30.i1.pp598-605.

[16] A. Akgundogdu, "Detection of pneumonia in chest X-ray images by using 2D discrete wavelet feature extraction with random forest," *International Journal of Imaging Systems and Technology*, vol. 31, no. 1, pp. 82–93, Oct. 2021, doi: 10.1002/ima.22501.

[17] J. Ebiele, T. Ansah-Narh, S. Djiokap, E. Proven-Adzri, and M. Atemkeng, "Conventional machine learning based on feature engineering for detecting pneumonia from chest X-rays," in *ACM International Conference Proceeding Series*, Sep. 2020, pp. 149–155, doi: 10.1145/3410886.3410898.

[18] A. Manickam, J. Jiang, Y. Zhou, A. Sagar, R. Soundrapandiyan, and R. Dinesh Jackson Samuel, "Automated pneumonia detection on chest X-ray images: A deep learning approach with different optimizers and transfer learning architectures," *Measurement: Journal of the International Measurement Confederation*, vol. 184, p. 109953, Nov. 2021, doi: 10.1016/j.measurement.2021.109953.

[19] K. Fang, "Naive bayes image classification based on multiple features," *Computer Software and Media Applications*, vol. 5, no. 1, 2022.

[20] M. M. Hasan, M. Md. Jahangir Kabir, M. R. Haque, and M. Ahmed, "A combined approach using image processing and deep learning to detect pneumonia from chest x-ray image," in *3rd International Conference on Electrical, Computer and Telecommunication Engineering, ICECTE 2019*, Dec. 2019, pp. 89–92, doi: 10.1109/ICECTE48615.2019.9303543.

[21] O. M. E. Zein, M. M. Soliman, A. K. Elkholy, and N. I. Ghali, "Transfer learning based model for pneumonia detection in chest X-ray images," *International Journal of Intelligent Engineering and Systems*, vol. 14, no. 5, pp. 56–66, Oct. 2021, doi: 10.22266/ijies2021.1031.06.

[22] D. S. Kermany *et al.*, "Identifying medical diagnoses and treatable diseases by image-based deep learning," *Cell*, vol. 172, no. 5, pp. 1122-1131.e9, Feb. 2018, doi: 10.1016/j.cell.2018.02.010.

[23] K. Almezhghwi, S. Serte, and F. Al-Turjman, "Convolutional neural networks for the classification of chest X-rays in the IoT era," *Multimedia Tools and Applications*, vol. 80, no. 19, pp. 29051–29065, Jun. 2021, doi: 10.1007/s11042-021-10907-y.

[24] S. Showkat and S. Qureshi, "Efficacy of transfer learning-based ResNet models in chest X-ray image classification for detecting COVID-19 Pneumonia," *Chemometrics and Intelligent Laboratory Systems*, vol. 224, p. 104534, May 2022, doi: 10.1016/j.chemolab.2022.104534.

[25] J. Zhao, M. Li, W. Shi, Y. Miao, Z. Jiang, and B. Ji, "A deep learning method for classification of chest X-ray images," *Journal of Physics: Conference Series*, vol. 1848, no. 1, p. 12030, Apr. 2021, doi: 10.1088/1742-6596/1848/1/012030.

BIOGRAPHIES OF AUTHORS

Murthuja Pinjara is Research Scholar at Department of Computer Science, Sri Venkateshwara University, Tirupati, Andhra Pradesh, India. He received his Master degree in Computer Science and Applications (MCA) from Osmania University, Hyderabad, Telangana. His main research areas include image processing, pattern recognition, machine learning, and deep learning. He can be contacted at email: pmurthuja.mca@hotmail.com.

Dr. Anjan Babu G is working as Professor and Head of the Department of Computer Science, Sri Venkateshwara University, Tirupati. He did his Ph.D. in Computer Science from Sri Venkateshwara University, Tirupati. He presented more than 65 papers in National and International Conferences and published 65 papers in reputed journals. He is also guiding the students for Ph.D. in the areas like data mining, neural networks, software engineering, and graph databases. He can be contacted at email: gababu.apps@gmail.com.